

Numerical simulation guided design of novel experimental chamber used to assess the effectiveness of ventilation strategies with hygro-regulated air terminals

Jean Paul Harrouz^{1*}, Bassam Moujalled¹, Michel Ondarts², Benjamin Golly²,
Adeline Mélois¹, Gaelle Guyot¹, Jérémy Depoorter³

*1 BPE Research Team—Cerema
46, rue Saint-Théobald, 38080
L'Isle d'Abeau, France*

**Corresponding author: jean-
paul.harrouz@cerema.fr*

*2 LOCIE UMR 5271
Université Savoie Mont-
Blanc, CNRS, 73376
Le Bourget-du-Lac, France*

*3 ANJOS VENTILATION
Lot. Roche Blanche, 01230
Torcieu, France*

ABSTRACT

Ensuring acceptable indoor air quality (IAQ) is critical for managing built environments. This is done by ventilating spaces with outdoor air to keep indoor pollutants like CO₂, humidity, particulate matter, and VOCs within healthy levels. The effectiveness of ventilation strategies depends on factors like occupancy, pollutant types, and air terminal devices, which can be influenced by outdoor air quality, especially in urban areas with particulate matter and NO_x. Ventilation devices can operate with constant airflow or adjust based on occupancy. Demand-controlled ventilation, using indoor CO₂ levels as an indicator, is more energy-efficient than constant-flow methods. For over 40 years, humidity-sensitive terminals (HST) have been used in French homes, mainly characterized by their flowrate and humidity control, but rarely in terms of IAQ. To optimize IAQ at minimal energy cost, it's essential to understand how HSTs transfer indoor and outdoor pollutants. This study aims to design an experimental chamber to test ventilation strategies using HST. First, a literature review of the existing experimental chamber highlighted the limitations to be overcome by the current developed testing facility. Second, numerical models were developed on CONTAM and computational fluid dynamics (CFD) to guide the chamber design. On one hand, CONTAM model was used to determine the emission rates of pollutants and the corresponding sizing of the generators and the proper selection of the control equipment (sensors, mass flow controllers). On the other, the CFD model assisted in determining the appropriate location of these various instruments for better control as well as proper functioning of the experimental chamber.

KEYWORDS

Ventilation strategy, indoor air quality, environmental chamber, pollutant transfer, computational fluid dynamics

1 INTRODUCTION

Humans are spending more than 90 % of their times in enclosed indoor spaces, whose envelope have been constructed with increasing airtightness, especially residential buildings, to limit air leakage and reduce energy losses (Paukštys *et al.*, 2021). However, indoor air quality (IAQ) of these buildings is deteriorated due to reduced outdoor air intake, which dilutes and evacuates the indoor contaminants. The latter have adverse health effects on occupants if left untreated, and they consist of a wide range of gaseous and solid pollutants originating from various sources. Outdoor generated contaminants englobe combustion products such as NO_x and particulate matter (PM), whereas indoor generated contaminants come from building materials such as volatile organic compounds (VOCs) or from occupants themselves such as moisture and CO₂. Although these two species are not typical pollutants, their presence at inadequate concentrations have indirect implication on human health. Low relative humidity (RH) levels cause eye dryness and skin irritation, while high RH cause mould formation in building structure, leading to fungus growth and asthma reactions as well as affecting the perceived

thermal comfort (Du *et al.*, 2021). Moreover, high CO₂ levels reduce attention span and cognitive performance while increasing absenteeism and air staleness.

Accordingly, ventilation systems have been used to regulate the outdoor air flowrate introduced indoors to maintain these species concentrations within acceptable thresholds. Typical ventilation strategies adopted a constant outdoor air flowrate that is supplied to the space throughout the day. Such systems resulted in elevated energy consumption, which gave rise to demand-controlled ventilation (DCV) where the outdoor air is supplied based on occupants needs. This led to more energy saving by limiting the use ventilation system during unoccupied periods of the houses (Nielsen & Drivsholm, 2010). Such smart ventilation systems rely conventionally on indoor CO₂ levels as occupancy indicator, due to its association with human activities through breathing (Lu *et al.*, 2022). Nonetheless, residential houses may be subject to pollution episodes not related to human metabolic emissions such as cooking and laundry, but that emits high loads of moisture and increasing indoor RH. Therefore, adopted humidity-based demand-controlled ventilation (HDCV) becomes a more suitable smart ventilation system for residential buildings. In fact, HDCV has been considered the reference ventilation system in most European countries (Sowa & Mijakowski, 2020), especially in France where it has been used for more than 40 years (Mélois *et al.*, 2023). HDCV systems operate based on the sweeping mechanisms where mechanical exhaust fans creates negative pressure in the house, causing outdoor air to enter through trickle vents placed on main living quarters (living and bedrooms) and pass to utility rooms (kitchen, toilets and bathrooms) through undercuts in the partition doors. For effective operation, these systems employ humidity-sensitive terminals (HST) for air inlets and outlets placed in the main and utility rooms, respectively. Using humidity-responsive material, the area of HST passively increases with the indoor RH levels, allowing higher outdoor air to sweep the residential building.

These HDCV systems show promising potential in energy saving in reaching up to 60 % in various climate conditions through numerical simulations (Guyot *et al.*, 2017). However, their IAQ performance have not been totally characterized, and is conducted with respect to a limited number of pollutants. Sowa and Mijakowski (Sowa & Mijakowski, 2020) studied, using multizone model, the indoor CO₂ and humidity variations in dwellings using HDCV with HST, and showed the system ability to meet required RH levels at the expense of a slight increase in CO₂ levels to 1200 ppm. Afshari and Bergsøe (Afshari & Bergsoee, 2009) constructed a real-life scale dwelling to experimentally study the evolution of indoor generated gaseous contaminants (humidity, CO₂ and VOCs) only using a HDCV system controlled using RH sensors placed in the chambers instead of HST. Therefore, it is of interest to have a holistic understanding of the HDCV, especially using HST due to their practicality by eliminating the need for sensor placement, and complex ventilation control systems. In this regard, experimental investigations prove a crucial tool for the study of such terminals due to the complex physics involving pollutants transfer, especially PM subject to effect of deposition and resuspension along with the indoor air aerodynamics.

The objective of this work is thus to develop a novel real-life scale experimental chamber that replicates a typical French dwelling in the aim of evaluating the ventilation effectiveness of exhaust HDCV using HST with respect to outdoor- and indoor-sourced contaminants of gaseous and particulate nature. To better guide the chamber design, this work first presents a literature review of the existing experimental chamber in literature. Second, numerical simulations are used with both CONTAM multizone and detailed computational fluid dynamics (CFD) models. The numerical simulation helps in making preliminary decisions regarding the placement of the different species generation and measurement ports. CONTAM serves in assessing the chamber dynamic performance across various ventilation flowrates. This aids in calculating pollutant emission rates required to attain pre-defined levels and dimensioning diverse pollutant generators. CFD simulations enable the knowledge of the pollutants spatial distribution to ensure homogeneity of conditions in the buffer zone and determine the correct

sensors placement. This ensures reliable readings, reflecting the pollutant dispersion needed to evaluate the ventilation strategies effectiveness under various HST types and locations, building airtightness levels and interior zones connection types.

2 REVIEW OF EXPERIMENTAL CHAMBERS

In literature, many experimental chambers have been developed to study various facets of IAQ and/or various ventilation systems. Mahyuddin and Awbi (Mahyuddin & Awbi, 2010) used a 17.75 m³ testing chamber representing a classroom to study various recirculation air fraction in a mixing ventilation arrangement. Heiselberg and Perino (Heiselberg & Perino, 2010) and Najafi Ziarani *et al.* (Najafi Ziarani *et al.*, 2023) developed experimental chambers with volumes of 35.4 m³ and 15.4 m³, respectively, to study indoor room airing by natural ventilation and its implication on IAQ. Metabolic CO₂ concentration was used to calculate local ventilation effectiveness, mean age of air and air change rates, without considering the other pollutants, especially the adverse effects of natural ventilation in polluted outdoor environment.

Harb *et al.* (Harb *et al.*, 2016) developed an innovative 40 m³ experimental chamber (IRINA) containing a CO₂ source and a heated pressurized injection of vaporized VOCs. The chamber is equipped with gaseous analyzers to conduct various IAQ studies such as testing the reliability of electronic gas sensors (Caron *et al.*, 2016), characterizing gaseous emissions from typical household and construction material (Harb *et al.*, 2018; Thevenet *et al.*, 2018) and evaluating localized air treatment and purification systems (Harb *et al.*, 2020). It can be noted that the majority of these studies focuses on gaseous indoor pollutants, especially VOCs even though it is equipped with a particulate analyzer. Moreover, no ventilation system/strategy has been studied so far using the developed IRINA chamber.

Jurelionis *et al.* (Jurelionis *et al.*, 2015) developed an experimental office space of 35.8 m³ to test evacuation effectiveness of PM emitted from two different sources using various outdoor air flowrates and ventilation configurations (mixing, displacement). Li *et al.* (Li *et al.*, 2023) tested, in a 50 m³ chamber, the effectiveness of stratum ventilation in reducing the cross-contamination between infected and healthy occupants with PM emissions to represent bioaerosols emitted from coughing or sneezing. Although the findings of the study were insightful, the study was limited to singular and short PM injection that simulate instantaneous indoor PM source (bioaerosols), and did not consider the effect of varying ventilation flowrates on other contaminants. Ciuzas *et al.* (Ciuzas *et al.*, 2015) developed a 35.8 m³ test chamber representing a standard living room to study the dynamics of PM evolution from other indoor pollution episodes such as cooking, smoldering cigarettes, burning candles and household/beauty product sprays. They noticed that PM build-up depends on the source type, whereas PM decay is affected by the emission duration. However, the effect of the ventilation system was not evaluated with respect to different flowrates or air terminal configurations.

From the above literature review, it can be clearly outlined that the need for the current developed experimental chamber that overcomes the limitations in the existing chambers as summarized below:

- No exhaust-based ventilation system has been considered, only supply ventilation with different configurations (mixing, displacement, stratum),
- Studies were conducted at specific constant ventilation rates with absence to variable demand-controlled ventilation, especially based on indoor humidity,
- Indoor moisture transfer was neglected as the studies are conducted at constant RH levels,
- A single type of pollutants is considered at a time with the ventilation effectiveness calculated relative to the adopted pollutant instead of using more comprehensive IAQ indicators,
- Only indoor generated pollutants are studied and outdoor contaminants transfer is disregarded (use of filtered clean outdoor air).

3 CHAMBER DESCRIPTION

The experimental chamber is built inside an insulated and thermally conditioned hangar, acting as a thermostatic holding area with relatively controlled air conditions. The experimental chamber comprises three main zones, illustrated in Figure 1. Zone 1 acts as a buffer simulating the building exterior, where pollutants are generated and maintained at constant target levels. Air from the thermostatic holding area is filtered and introduced via a large air grill at the floor, ensures clean air entering the chamber through a high-efficiency filter. Zones 2 and 3 represent a typical French residence, with zone 2 as the main living area and zone 3 as the utility room. The experimental chamber is equipped with an HDCV system designed to extract simulated outdoor air from zone 1 into zone 2 via the inlet HST. To increase the modularity of the chamber design, three air inlets with individual opening and closing controls are installed at the interface between these zones. This setup allows for studying the effects of the number and placement of air inlets. Additionally, three modular leakage defects are installed in this interface to assess the impact of different building airtightness levels and shapes on the H-DCV system's effectiveness. These defects can adjust the opening area to provide zone 2 with an airtightness ranging from 0 to $1.2 \text{ m}^3/\text{h}\cdot\text{m}^2$ (air flowrate at 4 Pa per envelope area excluding lower floor), with a specific focus on achieving $0.6 \text{ m}^3/\text{h}\cdot\text{m}^2$, which aligns with the French EP regulation for single-family buildings (Moujalled & Mélois, 2023). The defects, which are rectangular and circular, are installed at 0.9 m and 0.2 m above the floor, respectively, to represent common air leakage sources such as windowsills and electrical outlets (Desmarais *et al.*, 1998). The main chamber zones (zones 2 and 3) are separated by a demountable wall that includes a standard door ($0.84 \times 2.04 \text{ m}^2$) with a 2-cm undercut, allowing the sweeping air to pass to zone 3 when the door is closed. This setup simulates the air passage in actual residences equipped with HDCV systems. Furthermore, the interface between these zones is demountable, transforming the main chamber into a single-room residence, another common configuration in France. This flexibility is crucial for simulating the effectiveness of HDCV systems when living quarters and utility rooms, particularly kitchens, are connected. Finally, an exhaust HST is installed in zone 3 to drive filtered air from the thermostatic holding area through the previous two zones. Zone 3 also accommodates transient pollutant emissions associated with human activities, such as cooking or showering.

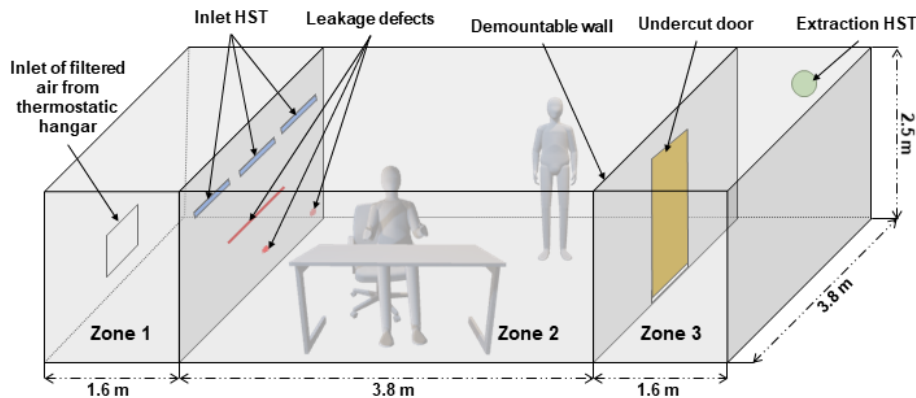


Figure 1: Schematic drawing of the current developed experimental chamber located in a thermostatic hangar

4 DESIGN REQUIREMENTS

Several requirements must be met to ensure the environmental chamber operates effectively and accurately represents actual H-DCV performance in homes. These requirements include

both physical aspects, such as geometry and envelope materials, and operational aspects, such as airtightness and pollutant generation.

The chamber volume affects airflow patterns and, consequently, the ventilation system's performance. In existing literature, chamber volumes range from a few litres to over 90 m³ (Harb et al., 2016). While small volume chambers facilitate easier control of operating conditions like temperature and humidity and faster pollutant homogenization, larger chambers (exceeding 30 m³) offer significant advantages despite technical and experimental challenges. Larger volumes allow for the study of commercial treatment systems, human exposure to air pollutants, and provide accurate surface-to-volume ratios and compliant air volumes to test ventilation systems. Therefore, the main chamber zones are designed with volumes of 36.1 m³ and 15.2 m³ for zones 2 and 3, respectively, with the dimensions presented in Figure 1, which indicates the smallest chamber volume possible while adhering the French codes of construction for minimal inhabitable areas (*Code de La Construction et de l'habitation - Légifrance*, n.d.) and ensuring a sensible chamber volume suitable for testing. Finally, the volume of zone 1 needs to be large enough to generate the simulated polluted outdoor air without requiring excessive preparation time to reach and homogenize contaminants at the desired concentration. Therefore, its volume was set to 15.2 m³, similar to zone 3. The filtered outdoor air inlet to zone 1 is positioned near the floor level and sized to maintain a supply air velocity of 0.1 – 0.2 m/s, akin to a displacement ventilation system, known to have minimal particle deposition due to its upward airflow pattern (Habchi et al., 2015). Axial fans are strategically placed near the floor level within the zone to aid mixing without disrupting the airflow pattern near the ceiling-level inlet HST. The direction of air blowing out of these fans is determined based on numerical simulations to ensure the highest homogeneous PM distribution.

Regarding the chamber inner surface material, stainless steel is used due to its non-adsorbing and chemically passive characteristics, eliminating any source/sink of undesired and unaccounted VOCs. Moreover, the chamber inner surfaces are electrically grounded to eliminate electrostatic forces that might affect PM deposition on the walls. The experimental chamber walls are also insulated with 8-cm of polystyrene to minimise the influence of surrounding air conditions on the inner zones. To better control indoor temperature and RH levels, separate air conditioning units are used: i) sensible cooling coil for air temperature control, ii) humidification wheel for moisture generation, and iii) dry airstream for indoor moisture reduction. The dry air is generated using a rotating desiccant wheel based on silica gel.

To assess the ventilation effectiveness of the HDVC system, various indoor pollutants are generated in the chamber. Outdoor-sourced species, such as NO_x and PM from combustion products, are chosen as they represent both gaseous and solid contaminants, enabling the study of different transport mechanisms. For indoor-sourced pollutants, moisture and CO₂ sources simulate occupant-related contaminants, including heat source to create thermal plumes affecting the airflow patterns. Additionally, VOCs like formaldehyde and toluene simulate emissions from materials, however, for this work, toluene has been selected due to the commercial availability of the chemical. Since VOCs are emitted from surfaces instead of punctual sources, the VOCs is released from a perforated tube placed along the zone wall to ensure a uniform injection of the gaseous product. Furthermore, PM is generated in zone 3 to replicate transient pollution episodes to mimic diverse human activities such as cooking, laundry, or showering and their associated contaminant emissions, as detailed in studies by Poirier *et al.* (Poirier *et al.*, 2021). The emission of PM is ensured by using an atomizer with saline solution. On one hand, atomization ensures the generation of electrically neutral particles compared to the use of dust generators, even though the latter offer easier control of emission rates. On the other hand, saline solutions are relative cheap (such as NaCl), which is crucial when the chamber is to be operated for prolonged durations, even though they provide a

polydisperse PM profile as opposed to the use of latex-based granules with more known monodisperse size distribution.

Moreover, the chamber maintains very low air permeability to minimize contaminant infiltration or exfiltration between zones and from its surroundings. This ensures accurate quantification of pollutant transport from desired sources without interference from unaccounted envelope leakage (Afshari & Bergsoee, 2009).

5 NUMERICAL METHODOLOGY

Numerical modelling and experiments complement each other: simulations help design experiments, while experimental data validates and calibrate the developed models. In this work, both CONTAM and Ansys Fluent are used to develop models for the new experimental chamber.

5.1 CONTAM model

CONTAM is a multizone airflow model that is commonly used to study pollutant transfer in indoor spaces due to its accuracy, ease of development, and low computational cost. It calculates airflows between zones and their surroundings, then determines pollutant concentrations based on these airflows. Each zone is treated as a homogeneous volume, connected to others through airflow paths like doors, windows, air terminals and leakage defects as shown in Figure 2. Additionally, pollutant emission for both gaseous and PM species are included in the model along with various sources/sinks types such as adsorption/desorption and chemical reactions for gases, and deposition/resuspension for particles (see Figure 2) (Szczepanik-Scislo & Scislo, 2021). The model uses mass balance to determine pollutant concentrations after calculating the interzonal airflows induced by their pressure differences using the Bernoulli's momentum balance and the orifice/power law for openings while also considering other factors such as thermal draft and wind pressure.

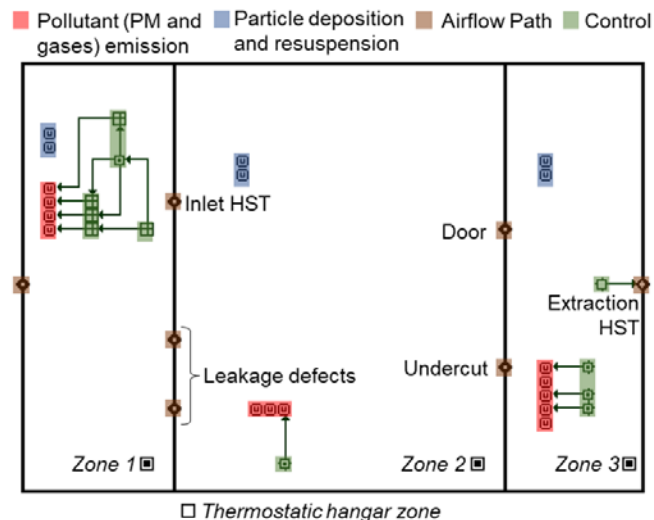


Figure 2: Layout of the environmental chamber used in the developed CONTAM model

5.2 CFD model

While CONTAM simulations provide reliable results for zonal pollutants concentrations, their assumption of well-mixed zones has limitations, particularly for PM, whose distribution is

affected by airflow patterns, gravitational settling, thermal stratification, and HST locations. CFD modelling using Ansys Fluent is thus adopted to better capture these different phenomena. The developed CFD model for the environmental chamber is depicted in Figure 3, along with the domain meshing at critical cross-sections, including the zones 1-2 interface, occupant manikin, and symmetry plane. In this study, two axial ventilators are used in zone 1 to ensure pollutant dispersion and mixing. These ventilators are placed near the floor at an elevation of 0.2 m to avoid disrupting the pressure distribution at the interface openings. The study explores two fan supply air directions to determine which provides the fastest and most uniform mixing. Pollutant generation locations are tested at two points: the centre of the room and the lateral walls perpendicular to the zone 1-2 interface, with injection points at a height of 0.5 m from the floor, as used by (Harb et al., 2016). To simulate occupants, two cylinders with a total area of 1.8 m² each are placed in zone 2, 0.5 m from the wall. Each cylinder has a circular opening of 192 mm² at a height of 1.2 m, representing a seated person's mouth, oriented to simulate two seated occupants facing away from the wall in a living room setting. Finally, an air-conditioning unit is modelled as a rectangular box with inlet and outlet openings at the top and bottom faces. This unit is added to zone 2, positioned 2.3 m above the floor on the wall behind the occupants and is operated to keep a constant temperature of 21 °C, similar to all inlet temperatures. This is adopted to reduce the effect of thermal stratification on PM transport and focus on that of the airflow pattern created by the HDCV system.

The domain is meshed using unstructured tetrahedral elements with varying face sizes for openings (1 mm) and walls (1 – 10 cm) along with inflation layers to ensure high mesh quality resulting with 2,187,559 elements and a y^+ below 1. Due to the high turbulence of the indoor airflow patterns, the CFD numerical model uses the two-equation RNG $k-\varepsilon$ model due to its robustness, accuracy, and low computational cost (Karam *et al.*, 2024). The model is used with enhanced wall treatment functions and full buoyancy effect consideration to better capture the boundary layer for reliable particle transport modelling (Katramiz *et al.*, 2022) along with the Boussinesq approximation. Discrete phase is simulated with the discrete random walk model to track the PM transport through a Lagrangian frame while accounting for local eddies. Only gravitational settling and drag forces are considered for the studied particle size ($> 0.1 \mu\text{m}$), which is assumed constant. The equations are discretized using the second-order upwind scheme, while the “PRESTO!” scheme is employed for pressure discretization. The coupling of the continuity and momentum equations is achieved using the SIMPLE algorithm. Convergence of the solution is reached when the residuals are less than 10^{-7} .

Although transient emissions can be simulated in the chamber, especially for humidity emissions that affect the HST openings, steady-state simulations are adopted in the CFD model at discrete points reflecting the transitional conditions of typical HST as function of RH levels. Finally, for the boundary conditions, all walls are considered adiabatic with reflect option for the PM, while a heat load of 39 W/m² and trap conditions are used for the cylinders. Pollutants emissions are simulated as velocity inlets with a unity mass fraction. Exhaust HST is also treated as inlet with negative velocity while the hangar air inlet is considered as a pressure inlet. Escape and reflect options are considered for the PM modelling, respectively. Inlet HST, leakage defects and door are considered as walls when they are closed and as interior otherwise.

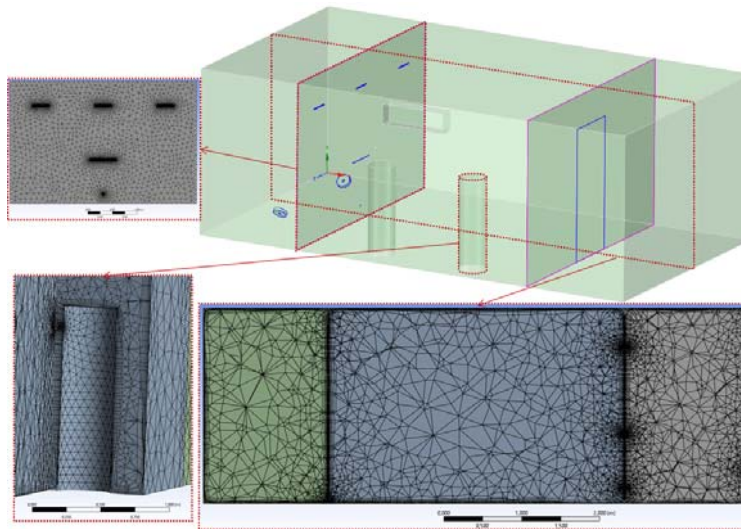


Figure 3: Illustration of the CFD computational domain with meshing at different cross-sections

6 PRELIMINARY RESULTS AND DISCUSSION

The developed models have been used to make preliminary decision regarding the chamber design, calculate the pollutants emission rates at different operating conditions needed to create simulated polluted air in zone 1. For this work, the “simulated outdoor air” of zone 1 is considered polluted with combustion products NO_x simulated with NO emission due to the lack of NO_2 tanks, as well as PM , with special focus on $\text{PM}_{2.5}$ and PM_{10} as they are the fractions of PM covered by IAQ regulations. The needed concentrations of these pollutants are $500 \mu\text{g}/\text{m}^3$, $300 \mu\text{g}/\text{m}^3$ and $150 \mu\text{g}/\text{m}^3$, respectively, in addition to a CO_2 concentration of 500 ppm. Another assumption that was adopted is to limit the preparation time of zone 1 to 15 minutes only while all openings are closed in the interface with zone 2. However, the axial fans are operated and an extraction flowrate is operated with exhaust to the outside near actual inlet at the ceiling levels. With these assumptions, the resulting emission rates of the pollutants in zone 1 are presented in Table 1, for three extraction flowrates typical for HST used in French dwellings (10, 45 and $135 \text{ m}^3/\text{h}$). Note that deposition and resuspension of PM are considered with velocities presented by (Thatcher & Layton, 1995). These parameters are to be calibrated in later work with the experimental results. The corresponding temporal variation of the pollutant concentrations in all zones are presented in Figure 4 for an operation of the chamber for one day, showcasing the stability of the established conditions, especially in zone 1. No emission scenario is included in the remaining zones at this stage.

As it can be seen, the emission rate of PM is expressed in terms of mass flowrate, however, the selection of the proper atomizer requires the knowledge of the particle count rate. For the conversion between the two rates, the particle volume and density are needed, and for this reason, the PM are assumed to have spherical shape with a density of $2 \text{ g}/\text{cm}^3$ (average density of typical salts used in such applications), which gives a combined particle flowrate between 9×10^4 and 5×10^5 particle/s, which falls within the range of the atomizer generation rates. Moreover, using the same logic for the conversion, the total particle count in the zone corresponding to the required target concentrations is around 1×10^7 particle/ m^3 , which is used to select the appropriate particle analyzer for the experimental chamber.

For the other pollutants, gas tanks are used with mass flowmeters to control the emission rates. Commercially, gas tanks for CO_2 and NO are available with high purity ($>99.99\%$), resulting in gas flowrates of 17 – 225 mLPM and 0.07 – 5.4 mLPM, respectively.

Table 1: Emission rates (mg/h) of pollutants into zone 1 to reach required concentrations of polluted outdoor air

Flowrate (m ³ /h)	CO ₂	NO	PM ₁₀	PM _{2.5}
10	1830	4.85	47.30	4.73
45	8235	21.83	58.00	10.00
135	24705	65.43	84.80	23.50

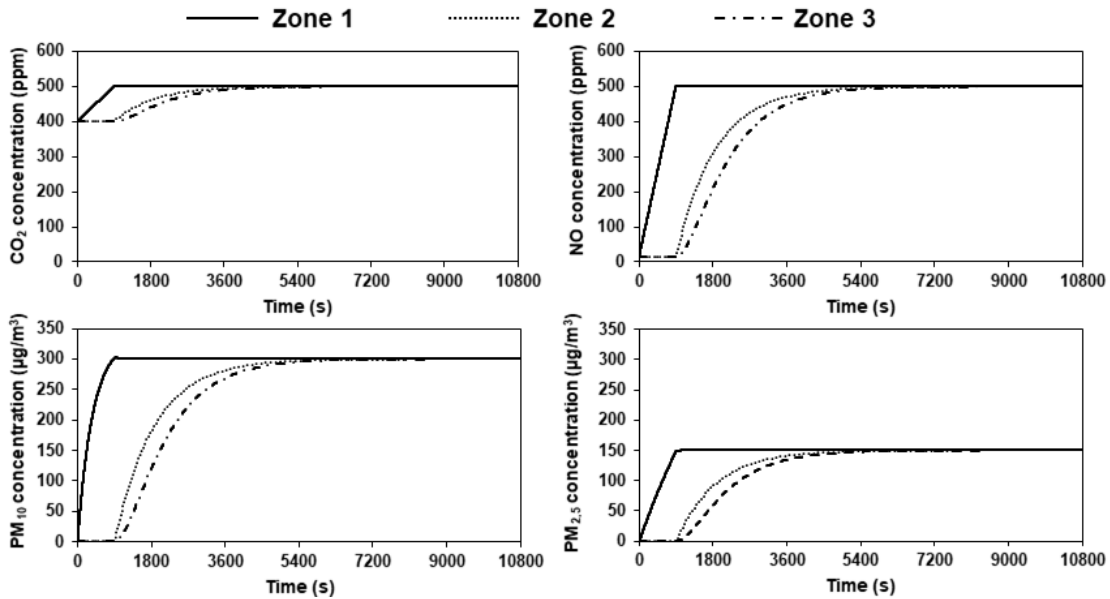


Figure 4: Pollutants concentration obtained in the experimental chamber zones using CONTAM

The obtained pollutants emission rates from CONTAM have been used as boundary conditions for the CFD model in two different configurations, center room and center wall emissions, along with two directions of the axial fans supply. The results of the simulations are presented in Figure 5 for the highest extraction flowrate of 135 m³/h, with an airtightness level of 0.6 m³/h·m² for the leakage defects. These conditions are selected to ensure uniform conditions at the different openings of the interface of zones 1 and 2. As it can be seen from Figure 5(a), the axial ventilators, with upward supply direction, creates additional turbulence in the zone with maximum velocities of 1 m/s along the fans axis, while maintaining low velocities below 0.15 m/s elsewhere. This was important to reduce their effect on the pressure field surrounding inlets while still ensuring enough mixing. Using this supply direction, it can be seen that emissions from the center of the wall provided higher homogeneity level compared to that in the center of the room, especially at the level of the inlet HST. In fact, a clear pollutant bypass can be clearly seen in Figure 5(b) when the emissions are room-centered caused by short-circuiting the air from the outdoor air inlet to the HST. Similar results have been obtained for PM concentrations where better mixed conditions is obtained in the case of wall-centered emissions. This can be attributed to the extraction of pollutants from the injection port near the wall directly into the stream of the fans before they are distributed. Hence, adopting wall emissions of the pollutants in zone 1 would be more suitable choice. Nonetheless, it should be noted that perfectly mixed and fully uniform PM distribution was not attained in either configuration, especially near the walls. This indicates that the sensors placement for the chamber control has a high influence on its behavior. For this reason, the control PM sensor were advised to be placed at the inlet HST, at midplane between the wall and the room center.

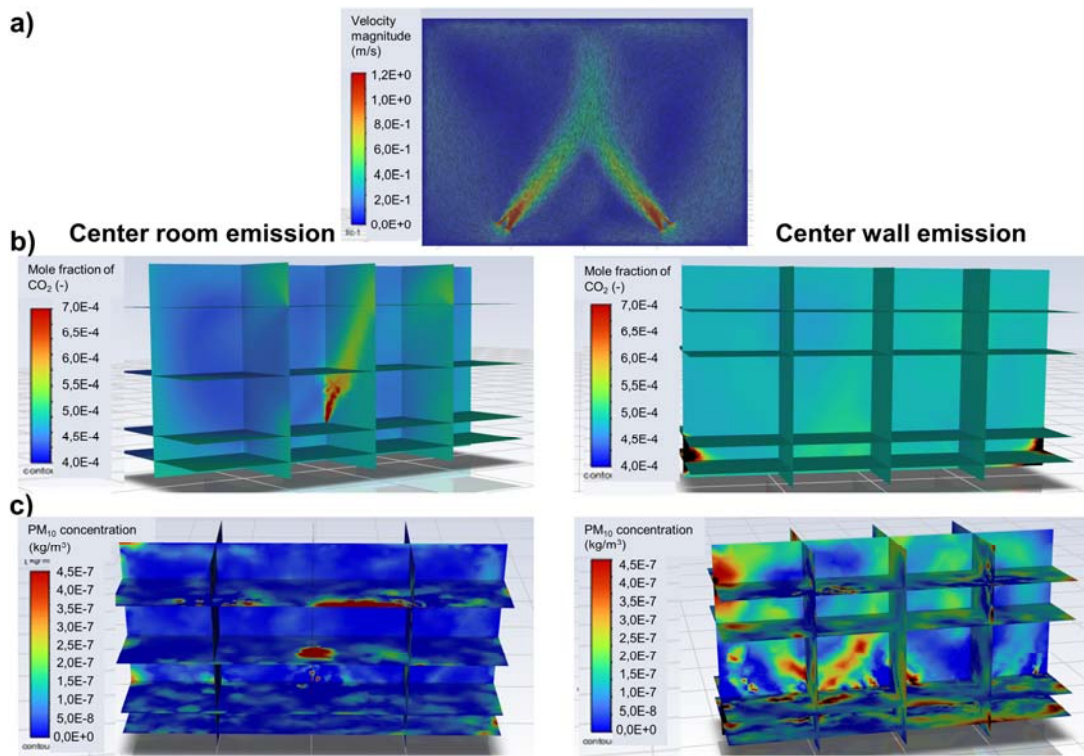


Figure 5: Results obtained using CFD simulations for upward supplying fans showing a) velocity profile, and the concentrations of b) CO₂ and c) PM₁₀ obtained from room and wall emissions

Using the pollutant emission scenario previously selected, the direction of the axial fans was reversed to provide downward supply of air, and the results are presented in Figure 6. As it can be seen, air velocities in the room center were below 0.15 m/s similar to the previous case. However, with the supply oriented to the floor, the Coandă effect is more pronounced, attaching thus the emitted pollutant jet to the adjacent wall, resulting in a higher local concentration. This can also be seen for PM concentrations were higher near the wall, along with a higher discrepancy between the PM concentration at the level of the different inlets. This was expected as supplying the air upwards, the fans extract the room air from the floor level and near wall and corners and supplied towards the room center; making thus this configuration more appropriate for the zone homogenization. Finally, compared between the two models, similar steady state conditions have been reached for gaseous components, while relatively larger differences ($< 400 \mu\text{g}/\text{m}^3$ combined concentration of PM_{2.5-10}), which highlights the need for models' calibration with experimental data from the chamber.

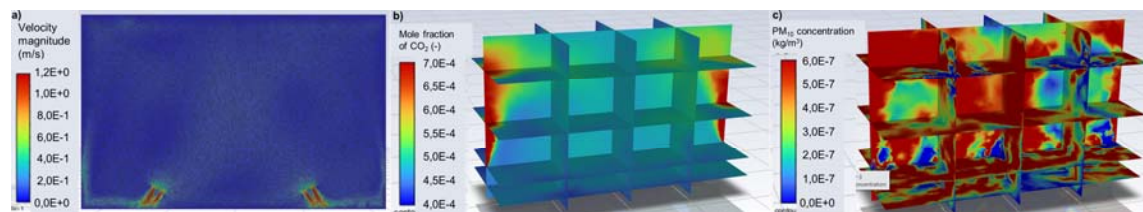


Figure 6: Results obtained using CFD simulations for downward supplying fans showing a) velocity profile, and the concentrations of b) CO₂ and c) PM₁₀ obtained from wall emissions

7 CONCLUSIONS

Maintaining acceptable IAQ is crucial for managing built environments, which is achieved by ventilating spaces with outdoor. In this regard, many ventilation systems have been developed

and tested. However, a literature review showed that there is a lack of experimental as well as numerical investigation concerning HDCV using HST that is considered as reference system in most European countries, especially France. For this reason, this work proposed the construction of a new experimental chamber, equipped with variety of equipment and with a high modularity. The chamber allows studying various HDCV strategies under typical operating conditions with respect to both outdoor- and indoor-generated pollutants, which has been shown lacking in the existing IAQ chambers. Numerical models were developed using CONTAM and CFD to guide the chamber design. The CONTAM model was used to determine pollutant emission rates, size the generators, and select the appropriate control equipment. Meanwhile, the CFD model helped determine the optimal placement of these instruments for better control and proper functioning of the experimental chamber.

8 REFERENCES

- Afshari, A., & Bergsoe, N. C. (2009). Humidity as a control parameter for ventilation. Phase 2: Development and testing of ventilation strategies in the laboratory. *Danish Building Research Institute*. <https://www.osti.gov/etdeweb/biblio/966475>
- Caron, A., Redon, N., Thevenet, F., Hanoune, B., & Coddeville, P. (2016). Performances and limitations of electronic gas sensors to investigate an indoor air quality event. *Building and Environment*, *107*, 19–28. <https://doi.org/10.1016/j.buildenv.2016.07.006>
- Ciuzas, D., Prasauskas, T., Krugly, E., Sidaraviciute, R., Jurelionis, A., Seduikyte, L., Kauneliene, V., Wierzbicka, A., & Martuzevicius, D. (2015). Characterization of indoor aerosol temporal variations for the real-time management of indoor air quality. *Atmospheric Environment*, *118*, 107–117. <https://doi.org/10.1016/j.atmosenv.2015.07.044>
- Code de la construction et de l'habitation—Légifrance*. (n.d.). Retrieved 3 June 2024, from https://www.legifrance.gouv.fr/codes/texte_lc/LEGITEXT000006074096
- Desmarais, G., Derome, D., & Fazio, P. (1998). *Experimental Setup for the Study of Air Leakage Patterns*.
- Du, C., Li, B., & Yu, W. (2021). Indoor mould exposure: Characteristics, influences and corresponding associations with built environment—A review. *Journal of Building Engineering*, *35*, 101983. <https://doi.org/10.1016/j.job.2020.101983>
- Guyot, G., Sherman, M., Walker, I., & Clark, J. D. (2017). *Residential smart ventilation: A review* (Research Report LBNL-2001056). LAWRENCE BERKELEY NATIONAL LABORATORY. <https://hal.science/hal-01670527>
- Habchi, C., Ghali, K., & Ghaddar, N. (2015). Displacement ventilation zonal model for particle distribution resulting from high momentum respiratory activities. *Building and Environment*, *90*, 1–14.
- Harb, P., Locoge, N., & Thevenet, F. (2018). Emissions and treatment of VOCs emitted from wood-based construction materials: Impact on indoor air quality. *Chemical Engineering Journal*, *354*, 641–652. <https://doi.org/10.1016/j.cej.2018.08.085>
- Harb, P., Locoge, N., & Thevenet, F. (2020). Treatment of household product emissions in indoor air: Real scale assessment of the removal processes. *Chemical Engineering Journal*, *380*, 122525. <https://doi.org/10.1016/j.cej.2019.122525>
- Harb, P., Sivachandiran, L., Gaudion, V., Thevenet, F., & Locoge, N. (2016). The 40 m³ Innovative experimental Room for INdoor Air studies (IRINA): Development and validations. *Chemical Engineering Journal*, *306*, 568–578. <https://doi.org/10.1016/j.cej.2016.07.102>
- Heiselberg, P., & Perino, M. (2010). Short-term airing by natural ventilation – implication on IAQ and thermal comfort. *Indoor Air*, *20*(2), 126–140. <https://doi.org/10.1111/j.1600-0668.2009.00630.x>
- Jurelionis, A., Gagytė, L., Prasauskas, T., Čiuzas, D., Krugly, E., Šeduikytė, L., & Martuzevičius, D. (2015). The impact of the air distribution method in ventilated rooms on the aerosol particle

- dispersion and removal: The experimental approach. *Energy and Buildings*, 86, 305–313. <https://doi.org/10.1016/j.enbuild.2014.10.014>
- Karam, J., Ghali, K., & Ghaddar, N. (2024). Resilience of Personalized Ventilation in Maintaining Acceptable Breathable Air Quality When Combined with Mixing Ventilation Subject to External Shocks. *Buildings*, 14(3), Article 3. <https://doi.org/10.3390/buildings14030654>
- Katramiz, E., Ghaddar, N., & Ghali, K. (2022). Novel personalized chair-ventilation design integrated with displacement ventilation for cross-contamination mitigation in classrooms. *Building and Environment*, 213, 108885. <https://doi.org/10.1016/j.buildenv.2022.108885>
- Li, H., Lan, Y., Liu, M., Kong, X., & Fan, M. (2023). Experimental research on the cross-infection control performance of different ventilation strategies. *Building and Environment*, 243, 110683. <https://doi.org/10.1016/j.buildenv.2023.110683>
- Lu, X., Pang, Z., Fu, Y., & O'Neill, Z. (2022). The nexus of the indoor CO₂ concentration and ventilation demands underlying CO₂-based demand-controlled ventilation in commercial buildings: A critical review. *Building and Environment*, 218, 109116. <https://doi.org/10.1016/j.buildenv.2022.109116>
- Mahyuddin, N., & Awbi, H. (2010). The spatial distribution of carbon dioxide in an environmental test chamber. *Building and Environment*, 45(9), 1993–2001. <https://doi.org/10.1016/j.buildenv.2010.02.001>
- Mélois, A., Legree, M., Sebastian Rios Mora, J., Depoorter, J., Jardinier, E., Berthin, S., Parsy, F., & Guyot, G. (2023). Durability of humidity-based ventilation components after 13 years of operation in French residential buildings – Assessment of components performance in laboratory. *Energy and Buildings*, 292, 113154. <https://doi.org/10.1016/j.enbuild.2023.113154>
- Moujalled, B., & Mélois, A. (2023). *Trends in building and ductwork airtightness in France*.
- Najafi Ziarani, N., Cook, M. J., & O'Sullivan, P. D. (2023). Experimental evaluation of airflow guiding components for wind-driven single-sided natural ventilation: A comparative study in a test chamber. *Energy and Buildings*, 300, 113627. <https://doi.org/10.1016/j.enbuild.2023.113627>
- Nielsen, T. R., & Drivsholm, C. (2010). Energy efficient demand controlled ventilation in single family houses. *Energy and Buildings*, 42(11), 1995–1998. <https://doi.org/10.1016/j.enbuild.2010.06.006>
- Paukštys, V., Cinelis, G., Mockienė, J., & Daukšys, M. (2021). Airtightness and Heat Energy Loss of Mid-Size Terraced Houses Built of Different Construction Materials. *Energies*, 14(19), Article 19. <https://doi.org/10.3390/en14196367>
- Poirier, B., Guyot, G., Geoffroy, H., Woloszyn, M., Ondarts, M., & Gonze, E. (2021). Pollutants emission scenarios for residential ventilation performance assessment. A review. *Journal of Building Engineering*, 42, 102488. <https://doi.org/10.1016/j.jobbe.2021.102488>
- Sowa, J., & Mijakowski, M. (2020). Humidity-Sensitive, Demand-Controlled Ventilation Applied to Multiunit Residential Building—Performance and Energy Consumption in Dfb Continental Climate. *Energies*, 13(24), Article 24. <https://doi.org/10.3390/en13246669>
- Szczepanik-Scislo, N., & Scislo, L. (2021). Comparison of CFD and Multizone Modeling from Contaminant Migration from a Household Gas Furnace. *Atmosphere*, 12(1), Article 1. <https://doi.org/10.3390/atmos12010079>
- Thatcher, T. L., & Layton, D. W. (1995). Deposition, resuspension, and penetration of particles within a residence. *Atmospheric Environment*, 29(13), 1487–1497. [https://doi.org/10.1016/1352-2310\(95\)00016-R](https://doi.org/10.1016/1352-2310(95)00016-R)
- Thevenet, F., Debono, O., Rizk, M., Caron, F., Verrièle, M., & Locoge, N. (2018). VOC uptakes on gypsum boards: Sorption performances and impact on indoor air quality. *Building and Environment*, 137, 138–146. <https://doi.org/10.1016/j.buildenv.2018.04.011>